A Comparison of DMPC- and DLPE-Based Lipid Bilayers

K. V. Damodaran and Kenneth M. Merz, Jr.
Department of Chemistry, 152 Davey Laboratory, The Pennsylvania State University, University Park, Pennsylvania 16802 USA

ABSTRACT A 250 ps molecular dynamics simulation of the dimyristoylphosphatidylcholine (DMPC)-based lipid bilayer, including explicit water molecules, is reported. The solvent environment of the head groups and other structural properties of the bilayer have been analyzed and compared with experimental results as well as our previous simulation of the dilauroylphosphatidylethanolamine (DLPE)-based bilayer. From this comparison we find that the solvent structure around the DMPC head group (clathrate shell) is significantly different than that around the DLPE head group (typical hydrogen bonding interactions). We have modeled the probable relationship between the different solvent environments around the R-$N(CH_3)_3^+$ (DMPC) and R-NH_3^+ (DLPE) head groups and the different interlammelar distances in these systems by performing potential of mean force (PMF) simulations on two $N(CH_3)_4^+$ and NH_4^+ ions in water. From the PMF simulations it appears that the differences in the hydration of the DMPC and DLPE head groups is not responsible for the differences in the hydration force observed for these systems. We also find that the orientational polarization of DLPE and DMPC is similar, which suggests that solvent polarization is not responsible for the differences in the hydration repulsion behavior observed in these systems. We also examined the order parameters for DMPC and found them to be in reasonable agreement with experiment. Given the different characteristics of the DLPE and DMPC head groups, we suggest an explanation of the differences in the interlammellar spacings of bilayers composed of these like-charged lipids. From our DLPE simulations we find that the R-NH_3^+ head groups can interact with the nonesterified oxygens of the phosphate group in an intraleaflet or an interleaflet manner. For the latter a "cross link" between two leaflets can be formed, which causes a stabilization of the interlamellar spacings at fairly short distances. Moreover, due to the strong intraleaflet interaction we find that the DLPE interface is relatively "flat" (as opposed to DMPC-based bilayers), which results in a surface that has regions of positive and negative charge that reside in the same plane along the bilayer normal. Based on this we propose that the DLPE bilayer interface can correlate itself with another DLPE interface by alignment of the regions of positive (or negative) charge on one leaflet with the opposite charges on the opposing leaflet.

INTRODUCTION

A molecular level description of the structure and dynamics of lipid bilayers will enhance our understanding of many important membrane functions. A variety of experimental techniques have been applied to investigate the structure, dynamics, and function of natural biomembranes and model lipid bilayers (Gennis, 1989). The structure and dynamics of dimyristoylphosphatidylcholine (DMPC)- and dilauroylphosphatidylethanolamine (DLPE)-based lipid bilayers have been investigated, at various degrees of hydration, by a number of experimental techniques in order to obtain critical information regarding the shape, hydration level, etc. of these membranes (Seelig and Seelig, 1974; Janiak, Small et al., 1979; Pearson and Pascher, 1979; Hauser et al., 1981; Blume, 1983; Cevc and Marsh, 1985; McIntosh and Simon, 1986; Yeagle and Sen, 1986). For example, it is known that a DMPC-based lipid bilayer has a gel to liquid crystalline transition temperature of 297 K and that the liquid crystalline phase of this bilayer absorbs 25–30 water molecules and has an area per lipid of 60–70 $Å^2$ in its fully hydrated state (Janiak et al., 1979; Hauser et al., 1981). Moreover, NMR data suggest that in the presence of excess water, water molecules bound to the lipid head groups exist in rapid equilibrium with bulk water (Salsbury, 1973; Finer and Darke, 1974). On the other hand, DLPE has a relatively smaller head group and is solvated by relatively smaller number of water molecules (McIntosh and Simon, 1986). Furthermore, the ammonium hydrogens of DLPE participate in hydrogen bonding with water as well as the nonesterified oxygens on the phosphate group of neighboring lipids. These features give rise to relatively smaller area per lipid for DLPE in the liquid crystalline state (~50 $Å^2$/lipid).

It is known that bilayers separated by solvent molecules repel each other to varying degrees. The repulsive force is known as the solvation pressure, or hydration pressure when the solvent is water (Rand and Parsegian, 1992). The hydration repulsion decays exponentially with the bilayer separation with a decay constant that depends on the packing density of the solvent (McIntosh et al., 1989). Simon and McIntosh (1989) have shown that the solvation pressure depends on the dipole potential due to the lipid head groups and the oriented solvent molecules in the interface. However, molecular dynamics (MD) simulations of model phosphatidylcholine (PC) (Kjellander and Marcelja, 1985) and phosphatidylethanolamine (PE) (Berkowitz and Raghavan, 1991) systems in water did not show an exponential decay of the orientational polarization. Israelachvili and Wennerstrom (1990) have given an alternative interpretation of these repulsive forces in terms of entropic forces arising from the confinement of thermally excited undulations of the bilayer

Received for publication 20 September 1993 and in final form 12 November 1993.

Address reprint requests to Kenneth M. Werz, Jr., Department of Chemistry, 152 Davey Laboratory, The Pennsylvania State University, University Park, PA 16802. Tel.: 814-865-3623; Fax: 814-865-8403; E-mail: merz@retina.chem.psu.edu.

0006-3495/94/04/1076/12 $2.00

surfaces into a small region as the two membranes approach. They suggest that the solvent plays only a minor role in the observed bilayer repulsion.

Computer simulations using molecular dynamics and Monte Carlo techniques have proved to be very powerful for studying the structure and dynamics of complex biological systems at the atomic level (McCammon and Harvey, 1987). Recently these techniques have been applied successfully to simulate lipid bilayers (Scott, 1977; Scott and Cherng, 1978; van der Ploeg and Berendsen, 1982, 1983; Scott, 1986; Pastor et al., 1988; Scott and Kalaskar, 1989; Brasseur, 1990; Berkowitz and Raghavan, 1991; De Loof, 1991; Pastor et al., 1991; Raghavan et al., 1992; Alper et al., 1993; Heller et al., 1993). Although very long simulations are required to examine phenomena like lipid diffusion, insights into many structural and dynamical features can be obtained from shorter simulations of several hundreds of ps. Monte Carlo simulations of lipid bilayers and lipid-protein interactions by Scott and co-workers (Scott, 1977; Scott and Cherng, 1978; Scott, 1986; Scott and Kalaskar, 1989), and the MD simulations by Berendsen and co-workers (van der Ploeg and Berendsen, 1983; Egberts and Berendsen, 1988) are notable in this regard. More recently, long MD simulations using detailed representations of the lipid and solvent environments have been performed for DMPC-based bilayers by Stouch (1993). The order parameter profiles calculated in these simulations showed good agreement with experimental results. We have reported an MD simulation of a DLPE-based bilayer wherein the structure and dynamics of the head group and hydrocarbon chains were examined (Damodaran et al., 1992). Furthermore, the structure of water near the lipid head groups was also studied with the help of various radial distribution functions. Brownian dynamics and stochastic boundary molecular dynamics methods have also been applied for investigating lipid bilayers (Pastor et al., 1988; De Loof, 1991; Pastor et al., 1991). These techniques are particularly suitable for investigating long-time dynamics, because simulation times of several hundreds of nanoseconds are possible (Pastor et al., 1988; De Loof, 1991; Pastor et al., 1991).

Among the lipids with neutral head groups, it has been observed that lipids with PC head groups tend to hydrate more and have large interlamellar solvent regions when compared to lipids with PE head groups (McIntosh and Simon, 1986; McIntosh, 1986; Rand and Parsegian, 1992). In a recent communication we have compared the head group-water interactions and head groups dynamics in DMPC and DLPE using MD simulations (Damodaran and Merz, 1993). The water structures around the head groups in these two systems are significantly different. The hydrophobic trimethylammonium groups of DMPC induce formation of clathrates in the nearby water molecules, whereas the ammonium groups in DLPE hydrogen bond to water oxygens. However, the different solvent orderings in these systems do not give rise to significantly different orientational polarization.

In this report we discuss the question of solvent ordering on the hydration repulsion in these systems. To further investigate the implications of the different solvent ordering on the hydration repulsion, we have performed potential of mean force (PMF) calculations of the representative structural groups in water, which are also discussed in the following sections.

MATERIALS AND METHODS

The model

In the crystalline state, DMPC has a surface area of ~39 Å^2 per lipid, and the alkyl chains are in the fully extended (*all trans*) state. Moreover, in the crystalline state of DMPC the lipids are all ordered along their long axis in the same manner. On going from the crystalline state to the gel state (L_β) the area per lipid increases, and the alkyl chains start to form *gauche* defects. The gel to liquid crystalline phase (L_α) transition is also accompanied by an increase in the surface area per lipid and a thinning of the bilayer due to the formation of extensive *gauche* defects. Thus, the high temperature L_α phase is characterized by considerable structural disorder. In our earlier simulation of the L_α phase of DMPC we used the crystal structure with lipid-lipid spacings increased proportionally in order to obtain the required surface area (Damodaran and Merz, 1993). These models showed very large collective tilting that resulted in very little van der Waals contacts between the lipids in the two monolayers. This was caused by the fact that the lipids were ordered along their long axis in a similar manner to what is seen in the crystal structure of DMPC. This was overcome in the present model by assigning a random orientation about the long axis in the plane of the bilayer for each lipid. Care was taken during the placement of each lipid to avoid any bad van der Waals contacts that could give rise to very large gradients/forces during the minimization and equilibration phases. Each monolayer is composed of 16 lipid molecules with a surface area of ~68 Å^2/lipid (Rand, 1981). The head groups of the two leaflets face each other at the center of the computational cell. With periodic boundary conditions, this simulates a multilamellar lipid bilayer with the hydrocarbons of the monolayers in contact. All methyl and methylene groups in the lipid except the methyl groups in the choline head groups were represented as united atoms. The bilayer was solvated by adding 861 SPC/E water molecules (Berendsen et al., 1987) (~27 waters/lipid) in the head group region of the computational box.

Potential parameters

Partial charges for the lipid atoms were obtained using STO-3G* electrostatic potential fitting on the entire DMPC molecule (Merz, 1992). These charges are given in Table 1 along with the structure and numbering scheme for DMPC. DLPE has an ammonium head group (RNH_3^+) instead of a choline head group ($RN(CH_3)_3^+$) and has alkyl chains that are 11 carbon atoms long instead of 13. Bond, angle, and dihedral parameters were taken from the AMBER force field (Weiner et al., 1984, 1986). The van der Waals interactions were represented by the OPLS parameter set (Jorgensen and Tirado-Rives, 1988) where the 1–4 (i.e., atoms connected through three covalent bonds) electrostatic and van der Waals interactions were reduced by a factor of 2 and 8, respectively (Jorgensen and Tirado-Rives, 1988).

Computational details

Molecular dynamics simulations were performed using the AMBER 4.0 package (Pearlman et al., 1991). All of the simulations were done at 315 K, well above the gel-to-liquid crystalline phase transition temperature (T_c = 297), using a temperature relaxation time constant of 0.20 ps applied separately to the lipid and water molecules (Berendsen et al., 1984). SHAKE (Ryckaert et al., 1977) was used to constrain all bond lengths to their equilibrium values in conjunction with a time step of 1.5 fs. We have used constant volume periodic boundary conditions. A residue-based nonbond pairlist with a cutoff distance of 13.5 Å was used. Thus, if any two lipid atoms are within the cutoff, all of the interactions between the two lipids are calculated.

TABLE 1 STO-3G ESP-Derived Charges for DMPC

Atom	Charge	Atom	Charge	Atom	Charge
N	0.0426	O2	−0.5491	C45	0.0064
C1	−0.2230	C12	0.2101	C46	−0.0125
H1	0.1370	C13	0.2231	O7	−0.4631
H2	0.1370	C30	0.3200	C16	0.5714
H3	0.1370	O5	−0.4631	O8	−0.4548
C2	−0.2230	C32	0.5714	C17	0.0064
H4	0.1370	O6	−0.4548	C18	0.0064
H5	0.1370	C34	0.0064	C19	0.0064
H6	0.1370	C35	0.0064	C20	0.0064
C3	−0.2230	C36	0.0064	C21	0.0064
H7	0.1370	C37	0.0064	C22	0.0064
H8	0.1370	C38	0.0064	C23	0.0064
H9	0.1370	C39	0.0064	C24	0.0064
C4	0.2527	C40	0.0064	C25	0.0064
C5	0.1876	C41	0.0064	C26	0.0064
O1	−0.5491	C42	0.0064	C27	0.0064
P	1.2855	C43	0.0064	C28	0.0064
O3	−0.7115	C44	0.0064	C29	−0.0125
O4	−0.7115				

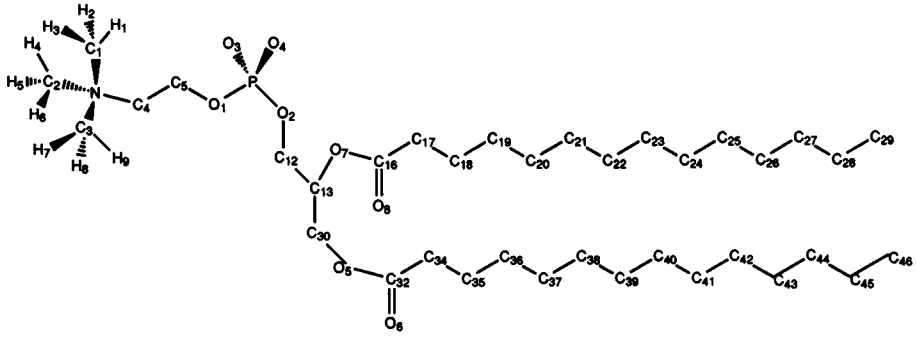

An initial 60 ps MD simulation was performed for equilibration of the system. Subsequently, the atomic coordinates and velocities were collected every 20 MD steps (0.030 ps) for 190 ps. The trajectory thus generated was used in the analyses described below. In some of these analyses, we have included results calculated for DLPE, using a trajectory from our earlier work (Damodaran et al., 1992). We have calculated probability distributions for different regions of the lipid bilayer and solvent molecules, pair distribution functions ($g(r)$) to evaluate the solvent structure surrounding the lipid head group region and the distribution of the alkyl chain tilt. We have also calculated the molecular order parameter profile for the alkyl carbon atoms. The dynamics of the system has been studied using velocity autocorrelation functions and mean square displacements.

Potential of mean force (PMF) simulations were done for two tetramethylammonium (TM) ions and two ammonium (AM) ions from a distance of 11 Å down to distances of contact repulsion. The model was built by solvating the two ions in a water box and equilibrating for 30 ps. A residue-based cutoff distance of 11 Å was used in both cases. At each point the configuration was equilibrated for 9 ps followed by sampling for 18 ps by moving the center of mass separation between the ions by 0.125 Å in the direction of approach. Double-wide sampling was used so that 0.250 Å could be sampled in each simulation. The ions were allowed to rotate about their center of mass during the MD simulation, and the simulations were performed at constant volume. For the TM ions a second simulation (hereafter referred to as TM-II) was performed using a solute-solute and solute-solvent cutoff distance of 15 Å and a solvent-solvent cut off distance of 11 Å, so that larger interionic separations could be probed. The PMF was calculated from the following relation (Buckner and Jorgensen, 1989; Dang and Kollman, 1990; Dang, 1992).

$$w(r) = -kT \ln\langle \exp\{-(H - H_0)/kT\}\rangle_0 \quad (1)$$

In Eq. 1 H_0 is the unperturbed Hamiltonian and H, the perturbed Hamiltonian, where the perturbation is introduced by changing the distance (r) between the two ions. The statistical averaging indicated by the angular brackets is done over the unperturbed state. The Hamiltonians can be broken into two contributions ($H = H_{vdw} + H_{elec}$; where H_{vdw} is the van der Waals component and H_{elec} is the electrostatic component of the Hamiltonians) to obtain insights into the relative importance of the electrostatic interactions and van der Waals interactions. This is not a rigorously correct assumption (i.e., $\Delta G \neq \Delta G_{elec} + \Delta G_{vdw}$), but we use this assumption to obtain qualitative insights into the relative importance of the electrostatic and van der Waals components in our PMF simulations.

RESULTS

Solvent order

The solvent order around the DLPE and DMPC head groups was studied using pair correlation functions ($g(r)$) from the head group atoms of the lipids to the oxygen and hydrogen atoms of the water molecules. The results are presented in Figs. 1–3. The number density of water used to evaluate the $g(r)$ was determined using the volume of the computational cell. Because this involves the large volume occupied by the bilayer (and no water), the $g(r)$ plots do not attain the traditional asymptotic value of 1.0. The $g(r)$ from the water molecules to the nitrogen atom in the head group of DLPE and DMPC are given in Fig. 1. For DLPE we have a traditional hydrogen bond between the ammonium head group and the surrounding water molecules, whereas in DMPC the

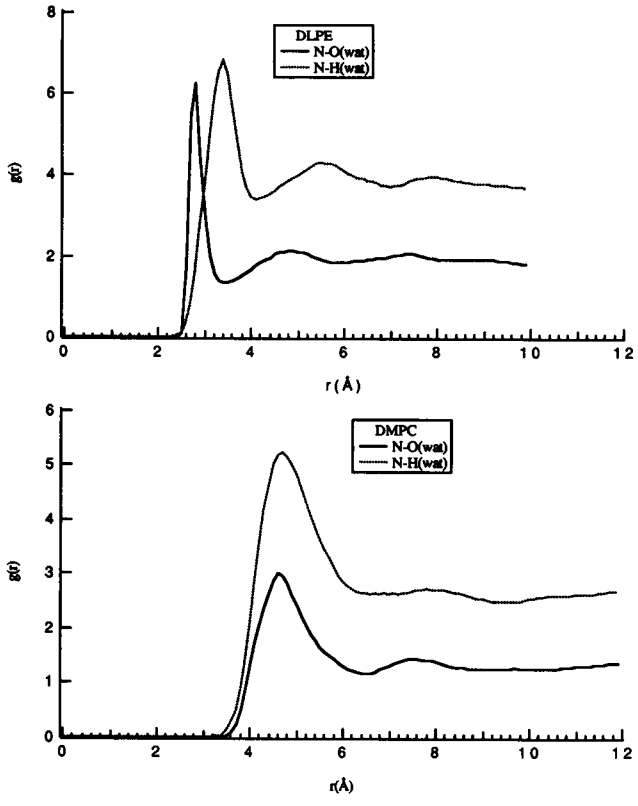

FIGURE 1 The N-O(wat) and N-H(wat) pair distribution functions for DLPE (*top*)- and DMPC (*bottom*)-based bilayers.

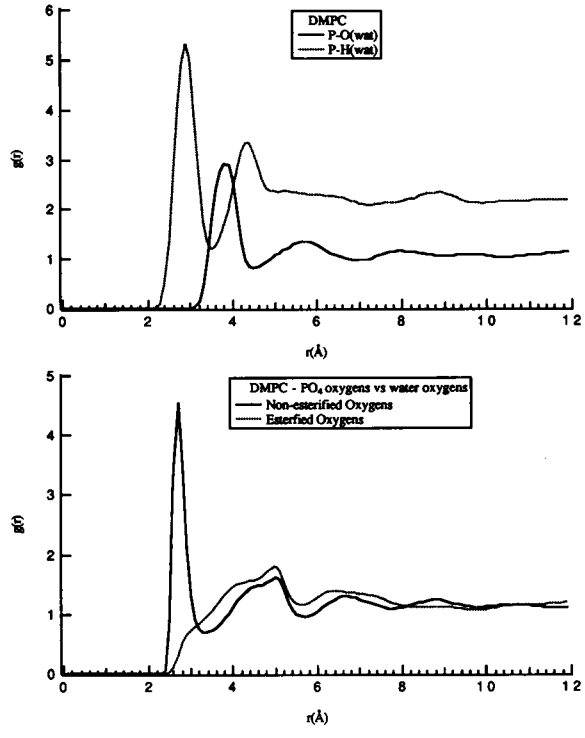

FIGURE 2 P-O(wat) and P-H(wat) radial distribution functions (*top*) and O(wat) pair distributions from the oxygens of the phosphate group (*bottom*) in DMPC.

trimethylammonium group, which is hydrophobic, induces the formation of clathrates in which the water molecules are hydrogen-bound among themselves. This is clearly seen on comparison of the $g(r)$ plots shown in Fig. 1. In the case of DLPE the first peaks in the N-O(WAT) and N-H(WAT) $g(r)$ plots appear at ~2.8 and ~3.6 Å, whereas the corresponding peaks in DMPC both appear at 4.6 Å. Because these water molecules are hydrogen-bound among themselves, there is no strong orientational preference towards the nitrogen, although the $-N(CH_3)_3^+$ group is positively charged.

The water distributions around the phosphate (see Fig. 2) and carbonyl groups (see Fig. 3) also indicate the presence of waters hydrogen bound to the nonesterified oxygens of the phosphate group and the carbonyl oxygens, respectively. The difference in the intensities of the pair distributions for the two carbonyl groups on the sn-1 and sn-2 chains is probably due to the different orientations of these chains (see Fig. 3). The esterified oxygens of the phosphate group are only weakly hydrogen-bonded as indicated in Fig. 2 (*bottom*), which is in contrast to the nonesterified oxygen atoms. Moreover, the ester oxygen atoms are also poorly hydrogen-bonded in comparison to the carbonyl of the ester. This is not unexpected given the reduced charges on the esterified oxygens relative to the nonesterified oxygens and carbonyl oxygens. From these simulations we find that water molecules only penetrate to about the carbonyl oxygen atom of the ester group. This is further verified in the probability distribution plots discussed below.

Potential of mean force

Because the radial distribution functions in Fig. 1 show significantly different solvent structures around DLPE and DMPC lipids, we have investigated the possible effects of the solvent ordering on the interactions between two TM ions and two AM ions using PMF simulations. These models represent, at least in an approximate manner, the interactions between opposing bilayer head groups in PC and PE bilayers. They do not, however, represent the effects due to the presence of the bilayer surface formed by the head groups and the confinement of the solvent molecules between these surfaces. Nonetheless, these simulations will provide insights into whether there is a greater repulsion between two AM and/or TM ions, which is arising from the differences in the head group solvation of these ions.

These PMF profiles are shown in Figs. 4–6. The PMF profiles were anchored to the corresponding profile for the primitive model. The profiles for the primitive model were obtained by treating the solvent water as a continuum with dielectric constant of 78.4. The total profiles for the AM ions and the TM ions shown in Figs. 4 and 5 are generally featureless and repulsive, which is similar to PMF profiles obtained for other cations using Monte Carlo, MD, and extended RISM calculations (Pettit and Rossky, 1986; Buckner

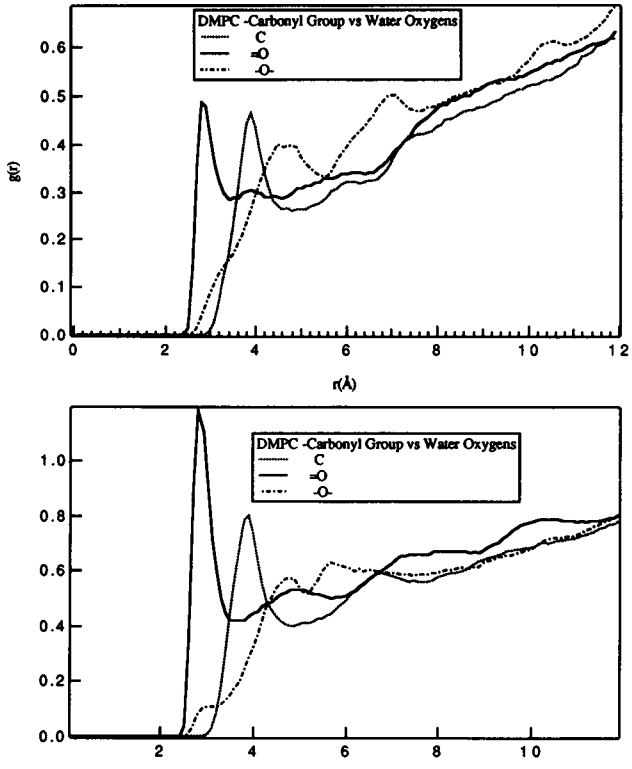

FIGURE 3 O(wat) pair distributions from the oxygens of the carbonyl group in DMPC. The sn-1 (*top*) and sn-2 (*bottom*) chains are given separately for clarity.

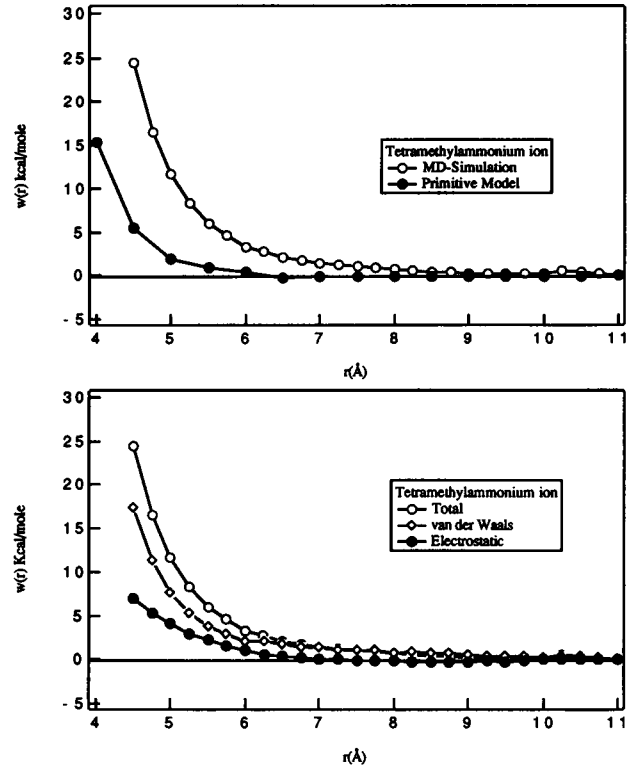

FIGURE 4 (*top*) The PMF profile for TM ions shown along with the primitive model. (*bottom*) The profiles obtained treating the van der Waals and electrostatic energies separately.

and Jorgensen, 1989; Dang and Pettit, 1990). Our profile for TM ions is similar to the one obtained by Buckner and Jorgensen (1989), although we have calculated the PMF for larger separations and have used a larger cut off distance for the nonbond interactions.

Both profiles are more repulsive than the primitive model. However, the closest distance of approach for TM ions is much larger (~5 Å) than that for the AM ions (~3 Å). We have also shown the profiles calculated from the van der Waals and electrostatic contributions to H_0 and H in Eq. 1. Although these individual contributions have only limited meaning, it is interesting to note that the van der Waals contribution to AM ions has a minimum at the contact distance while total profile is repulsive. This behavior is not observed for the TM ion.

Because of the size of the TM ions relative to the AM ions we decided to carry out a second PMF simulation where we extended the distance examined for the TM ions. This was done because for the TM ions we had barely reached the solvent separated point on the PMF profile when we used an 11-Å cutoff. In the case of the AM ions, which are smaller, we had passed the solvent separated point by several Ångstroms. once we reached the 11-Å point. The PMF profile obtained from simulation TM-II is given in Fig. 6 and is different from the profile for TM ions given in Fig. 5. The total profile is attractive up to ~9 Å, followed by a broad minimum until ~7 Å before becoming repulsive as the ions come into close contact. Differences in PMF profiles due to different truncation procedures have been reported previously by Huston and Rossky (1989). The profiles obtained considering the van der Waals and electrostatic components (compare Figs. 5 and 6) show that the van der Waals component behaves similarly in both cases, whereas the electrostatic part shows significantly different behavior. However, if one takes the TM-II profile and truncates it at the 11-Å point, one finds that the two profiles are more closely related than is evident. Nonetheless, the TM-II profile remains more attractive, but to a lesser extent. Overall, this suggests that for the large TM ion it is important to use larger cutoffs to determine whether a solvent separated minimum is present along the PMF profile. The differences observed could also be due to several other factors. The obvious reason for this is due to the slowly decaying nature of the electrostatic potential, which suggests that the 11-Å cutoff used in the first simulation does not adequately represent the electrostatic interaction for the larger TM ion. Mean square displacements (i.e., diffusion constant) of water molecules at a TM-TM separation of 8 Å calculated using a 45-ps trajectory showed lower values for the second simulation presumably due to more waters "bound" to the ions due the larger cutoff. Hence, with the larger cutoff distance we find that the solvent dynamics are significantly affected. Finally, the different cutoff distances used for solute-solute, solute-solvent (15 Å), and solvent-solvent (11 Å) interactions may have an effect on the PMF profile for the TM-II simulation. Nonetheless, it is our expectation that the TM-II profile is more realistic

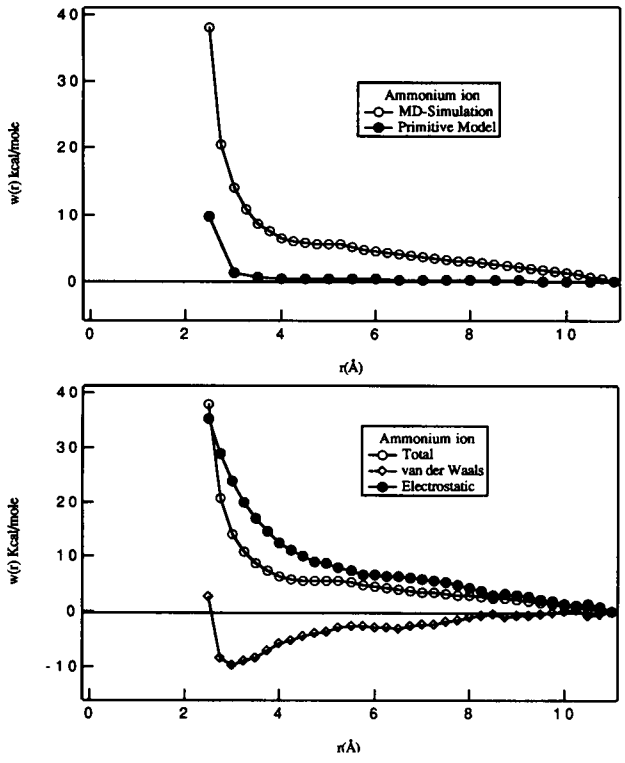

FIGURE 5 (*top*) The PMF profile for AM ions shown along with the primitive model. (*bottom*) The profiles obtained treating the van der Waals and electrostatic energies separately.

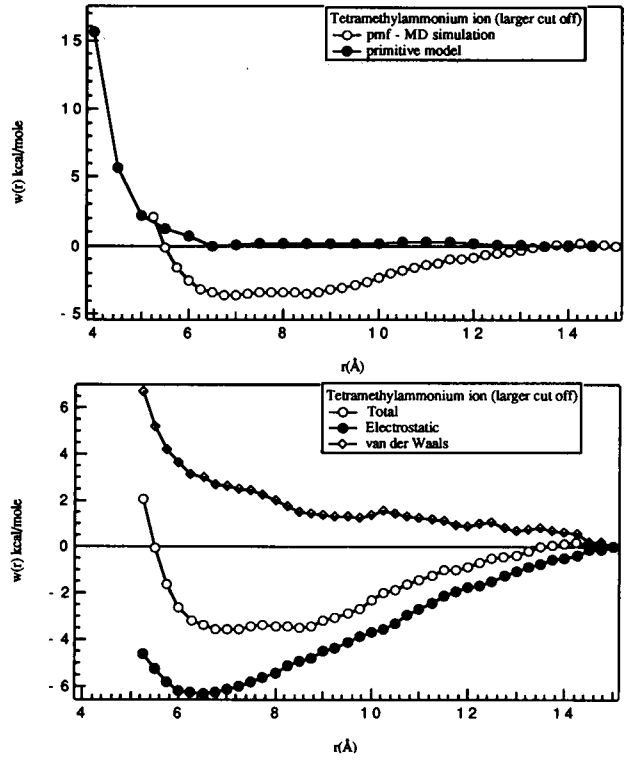

FIGURE 6 (*top*) The PMF profile for TM ions shown along with the primitive model using the larger cut off (for details see text). (*bottom*) The profiles obtained treating the van der Waals and electrostatic energies separately.

than the TM profile. Overall, this set of simulations also serves as another example of the sensitivity of the PMF on the simulation procedure (Huston and Rossky, 1989).

From the radial distribution functions calculated in the preceding section (see Fig. 1), we expected that the interaction between two AM ions versus that between two TM ions would be substantially different due to the observed differences in the solvation of these ions. However, the PMF profiles for AM (Fig. 5) and TM (Figs. 4 and 6) do not show any features directly attributable to the differences in the solvation of these two ions. Thus, the PMF results suggest that the different solvent structure in the interlamellar region (clathrate shell (DMPC) versus hydrogen bonding (DLPE)) plays only a minor role (if any) in the hydration repulsion. The differences in the distance of closest approach should be expected from size considerations (~3.5 Å for AM and ~6 Å for TM) for the two ions. From the behavior of the PMF profiles in conjunction with the probability distributions (see below) it appears that the larger interlamellar separation observed in PC-based bilayers is due to the steric repulsion of the choline head groups protruding into the solvent from opposing monolayers.

Singlet probability distributions

The probability distribution functions for various groups along the bilayer normal are shown in Fig. 7. Applying periodic boundary conditions in the direction of the bilayer normal shows that the alkyl chains have some degree of interdigitation. The peak-to-peak distances for the head groups ($R\text{-}NH_3^+$ and $R\text{-}N(CH_3)_3^+$ groups) in DLPE and DMPC are ~13 and ~22 Å, respectively, which are in reasonable agreement with those observed using electron density maps (13.1 and 25.4 Å, respectively) (McIntosh, 1990). The bilayer thicknesses for DLPE and DMPC estimated from the probability distributions are ~36.6 and 40.2 Å, respectively, which may be compared to the experimental values of 33.0 ± 0.60 Å for DLPE and 37.8 ± 0.80 Å for DMPC (McIntosh, 1990). It is interesting to note that in DMPC the choline head group distribution extends deep into the solvent region with respect to the phosphate group, whereas in DLPE the ethanolamine and phosphate distributions are at the same position. This is due to extensive hydrogen bond contacts between the ammonium group of ethanolamine and the phosphate oxygen atoms, which are not present in the DMPC-based bilayer. In the case of DLPE, the distributions for the ethanolamines show close contact between the two opposing leaflets, which indicates that hydrogen bonding is occurring between an ethanolamine head group (the ammonium group in particular) and the phosphate groups from the opposing leaflet. Wiener and White (1992) have studied the interface region in DOPC at 66% relative humidity, which gives some insight into the structure of the PC head group region. They have found the choline probability distribution and the phosphate probability distribution are shifted relative

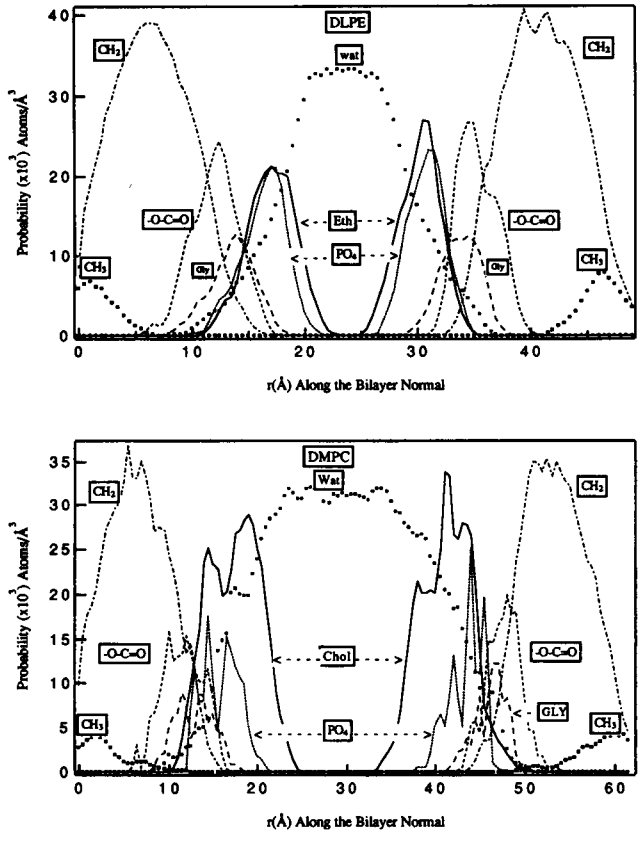

FIGURE 7 Probability distribution profiles for various regions of the lipid molecules and the solvent for DLPE (*top*) and DMPC (*bottom*). Abbreviations: Eth, ethanolamine; Gly, glycerol; Wat, water; Chol, choline.

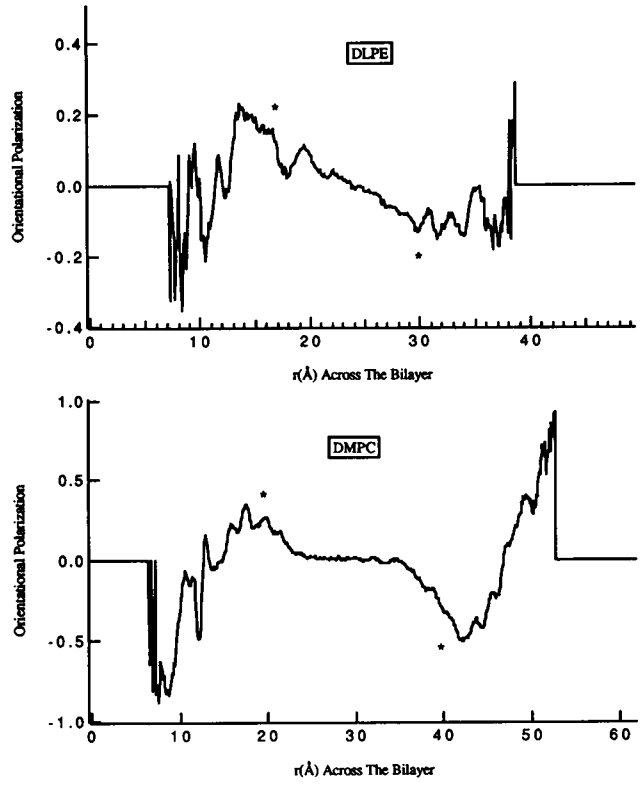

FIGURE 8 Orientational polarization profiles for DLPE (*top*)- and DMPC (*bottom*)-based bilayers. Note the differences in the scales of the two plots.

to one another as we have seen for DMPC. Unfortunately, we are unaware of any data on the PE interface region. The distributions also show the rough nature of the bilayer solvent interface. Penetration of water into the head group-solvent interface region until the carbonyl oxygens is also evident from the figure (Büldt et al., 1979). We also find that water penetration into the DMPC bilayer is more extensive than in the DLPE bilayer, presumably due to the larger area per lipid and lipid-lipid spacings in the former. Finally, we note that the distribution profiles are not symmetric, which is probably due to insufficient averaging.

Orientational polarization

We have calculated the orientational polarization profiles of the interlamellar water in DLPE and DMPC. Fig. 8 shows the polarization profiles along the bilayer normal. Because the interlamellar region is very thin in DLPE, most of the waters are bound to the head groups, and there is only a very small region that is similar to the bulk waters characterized by zero orientational polarization. The head group water interfaces, taken as the peak positions of the ethanolamine and choline probability distributions (discussed above) are marked in the figures. The decay of the polarization from this point into the solvent region could be fitted to an exponential with a decay length of 2.35 ± 0.25 Å ($R^2 \sim 0.84$) for DMPC. Furthermore, the polarization extends out from the surface of the two monolayers for ~7 Å. The polarization curve for DLPE shows spike-like features in the region of the phosphate and carbonyl groups due to water penetration. These waters are highly ordered due to hydrogen bonding. The profile for DMPC is smoother compared to DLPE, probably due to more water penetration into the interface region caused by a larger lipid-lipid spacing. We have also done a fit for DLPE, but this was only done for the leaflet on the right hand side of Fig. 8, because the leaflet on the left hand side was too oscillatory to fit accurately. A value of the decay length obtained in this way is 1.75 Å ($R^2 = 0.88$), and the polarization appears to extend out to ~7 Å, but becausee the bulk region is very small in our simulation, this latter value is uncertain.

From this analysis we find that the polarization profiles of DLPE and DMPC are similar, which suggests that solvent polarization is not responsible (nor is a suitable order parameter) for the hydration force differences seen in these systems.

Alkyl chain tilt

The distribution of the alkyl chain tilt in DLPE and DMPC simulations are shown in Fig. 9. These curves were obtained by averaging over the whole trajectory for both chains of lipids in the two monolayers. It is interesting to note that there are some chains, although less in number, which are almost parallel to the bilayer surface, that give rise to peak intensities

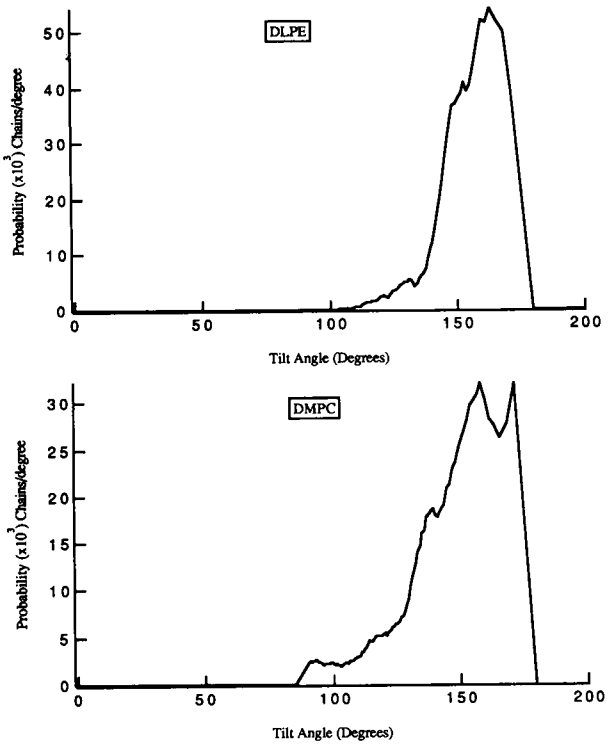

FIGURE 9 Distribution of the alkyl chain tilt with respect to the bilayer normal in DLPE (*top*) and DMPC (*bottom*).

near the 90° end of the plots. Our earlier model for DMPC, in which the crystal structure was used to generate the starting configuration, showed larger intensities in the low angle region of these plots. Moreover, visual examination showed that the tilt was collective in nature. Although the distributions in Fig. 9 do not distinguish between chains tilted in different directions, visual examinations confirm that there is no collective tilt, unlike the earlier DMPC model. We believe that this is due to the rotational disorder introduced in the starting structure. However, the head group and solvent environments have not changed as a result of this modification. For example, the head group-solvent radial distribution functions and the power spectrum of the head group motions were identical in both models (Damodaran and Merz, 1993).

Order parameters

The molecular long axis order parameters for the alkyl carbons were calculated from the relation

$$S_n = \tfrac{1}{2}\langle 3(\cos^2\beta_n - 1)\rangle \qquad (2)$$

where β_n is the angle between the bilayer normal and the vector joining carbons n-1 and n+1 in the alkyl chain (Pastor et al., 1988). Assuming an axial symmetry, the NMR order parameters can be obtained from the molecular order parameters by multiplying by 0.50 (Seelig, 1977). The calculated order parameters from the "crystalline" (Damodaran and Merz, 1993) and the random structure models are shown in Fig. 10 along with the experimental values for DPPC reported by Seelig and Seelig (1974). The order parameters have improved substantially. However, some features, like the characteristic dip at carbon position 3, have not been reproduced. This has also been observed by others (De Loof, 1991; Heller et al., 1993; Stouch, 1993) and may be due to the fact that the MD simulations run to date are fairly short (<1 ns), and effects like lipid protrusion, which might increase the flexibility of C3, are not adequately sampled. Of course, errors in the force field representation cannot be ruled out either. As shown by Seelig and Browning (Seelig and Browning, 1978)the order parameter profiles of different systems may be compared at their reduced temperatures $Tr = (T-Tc)/Tc$, where Tc is the gel-liquid crystalline phase transition temperature. The experimental values given in Fig. 10 are at lower Tr (0.05) than the calculated ones (0.06). Thus, the agreement with experimental results is better than what is apparent figure. The collective tilt of the alkyl chains, as described above, has affected the order parameters of the "crystalline" (Damodaran and Merz, 1993) model because the projection of a tilted segment onto the bilayer normal will be lower than a vertical one. The order parameters we observe are similar to those obtained from other MD simulations that have been reported in the literature (De Loof, 1991; Heller et al., 1993; Stouch, 1993).

Head group dynamics

We have analyzed the head group dynamics by determining the velocity autocorrelation functions (VAFs) for both DLPE and DMPC. The VAFs are given in Fig. 11 for the DMPC and DLPE head groups. The VAFs were calculated as

$$c(t) = \frac{\langle v(0)v(t)\rangle}{\langle v(0)v(0)\rangle} \qquad (3)$$

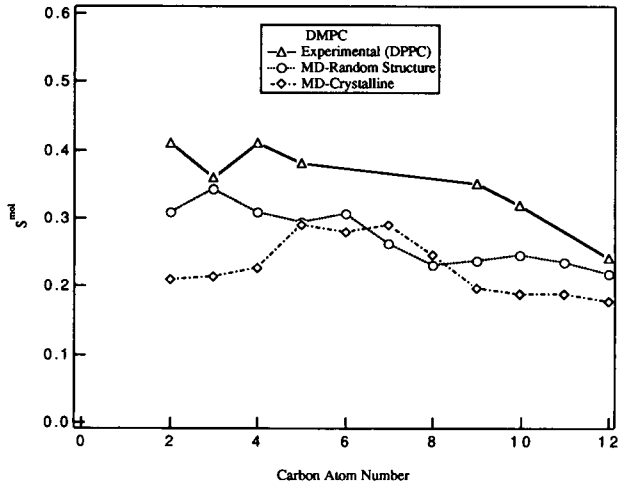

FIGURE 10 Molecular order parameters for the alkyl carbons calculated for DMPC. Experimental values are for DPPC.

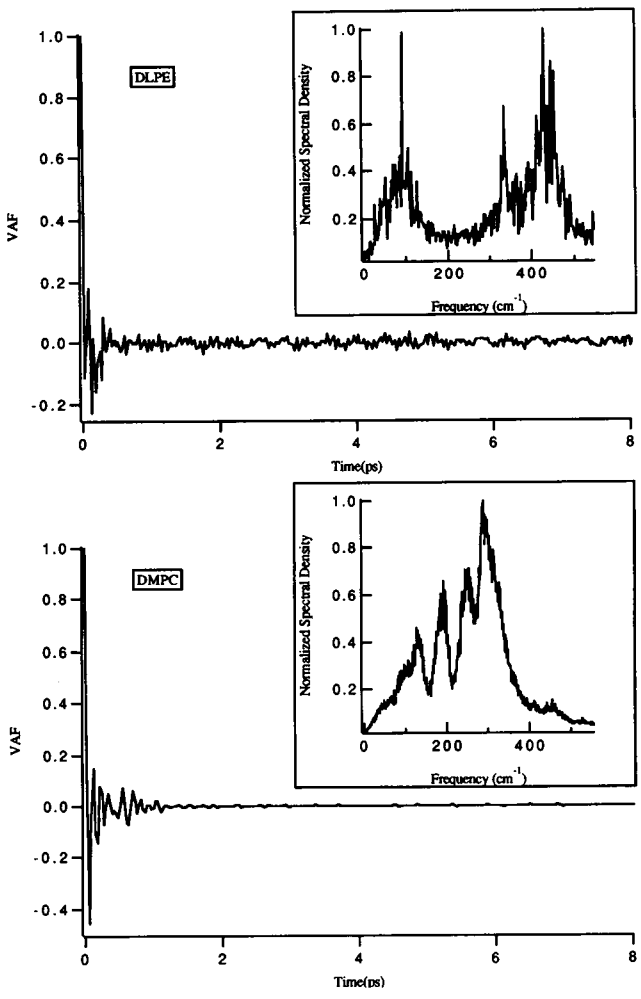

FIGURE 11 Velocity autocorrelation functions for the head groups of DLPE (*top*) and DMPC (*bottom*) based bilayers. The normalized power spectra are shown as insets.

and the spectral density function $I(\omega)$ was obtained as

$$I(\omega) = \int_0^{t_{max}} c(t)\cos(\omega t)\, dt. \qquad (4)$$

The angular brackets in Eq. 3 imply averaging the velocities (v) over the entire MD trajectory.

The VAFs of Fig. 11 clearly indicate the differences in head group dynamics due to the nature of head group-water and head group-head group interactions. The DLPE head groups encounter frequent collisions due to the formation and rupturing of hydrogen bonds with water and neighboring head groups. This results in a VAF that does not decay smoothly to zero as well as an power spectrum ($I(\omega)$) that is shifted to higher frequencies than for DMPC. The shifting of the power spectrum to higher frequencies indicates that the inter-head group and head group-solvent interactions are stronger for DLPE than they are for DMPC (differential rotational motion of R-NH_3^+ and R-$N(CH_3)_3^+$, and the greater mass of the latter head group may also play a role in the observed differences in the spectral densities). This is further manifested in the VAF for the DMPC head group where the motion decays to zero rapidly, indicating a much smoother motion. Clearly, the head group regions of these two lipids undergo significantly different motions relative to one another, with the DMPC head group being more conformationally flexible than the head group of DLPE. This observation could be important when considering the entropic confinement of head groups and its role in the hydration force. The present results suggest that the DMPC-based bilayer would experience a greater entropic penalty than the DLPE bilayer as a result of head group confinement (see Conclusions).

Water dynamics

We have analyzed the mobility of water by classifying them as bulk and bound, depending on their proximity to the lipid head group atoms. This analysis has already been reported for DLPE (Damodaran et al., 1992) as has an earlier one for DMPC using an earlier trajectory (Damodaran and Merz, 1993). In the case of DMPC we considered any water within 6 Å from *any* head group atom as a bound water and water molecules farther away from *all* head group atoms as bulk water. For DLPE we used a distance of 4 Å (the position of the first peak in the water-head group radial distribution function) (Damodaran et al., 1992). The probability distributions for the bound and bulk waters for DLPE and DMPC along the bilayer normal are shown in Fig. 12. The bound waters for DMPC are involved in a clathrate like structure while the bulk water molecules are involved in the interaction between each other and the clathrate shell (see Fig. 12, *bottom*). Note that the shapes of the regions containing the bulk and bound water molecules for DLPE and DMPC are quite complex, because of the nature of the surface formed by the lipid head groups and the fact that the disposition of the water-head group interactions are determined by this surface.

For DMPC we have calculated the mean square displacement and velocity autocorrelation functions for the bound and bulk waters separately (see Fig. 13). The DLPE values were reported previously (Damodaran et al., 1992). The bulk/bound status of the water molecules were updated every ps to account for the diffusion of water molecules between the bulk and bound regions. On an average, there were ~300 bulk waters (out of the total of 842 waters). The bound waters ($D = 1.5 \times 10^{-5}$ cm^2/s), as expected, show a lower diffusion coefficient and higher intensities in the high frequency region of the spectral density relative to the bulk water molecules ($D = 2.7 \times 10^{-5}$ cm^2/s). This behavior is essentially identical to that observed for DLPE (Damodaran et al., 1992). Note that SPC/E water has a diffusion constant of 2.5×10^{-5} cm^2/s at 300K (Berendsen et al., 1987).

CONCLUSIONS

From our simulations we have observed that the head group/water interactions in DLPE and DMPC-based bilayers have substantial differences. The formation of clathrate shells by

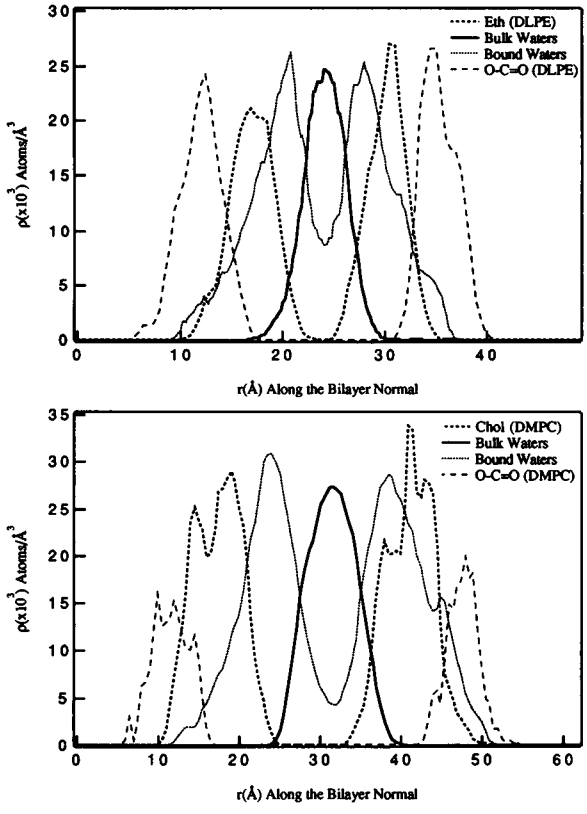

FIGURE 12 Probability distribution profiles for the bulk and bound waters in the DMPC (*top*)- and DLPE (*bottom*)-based bilayers.

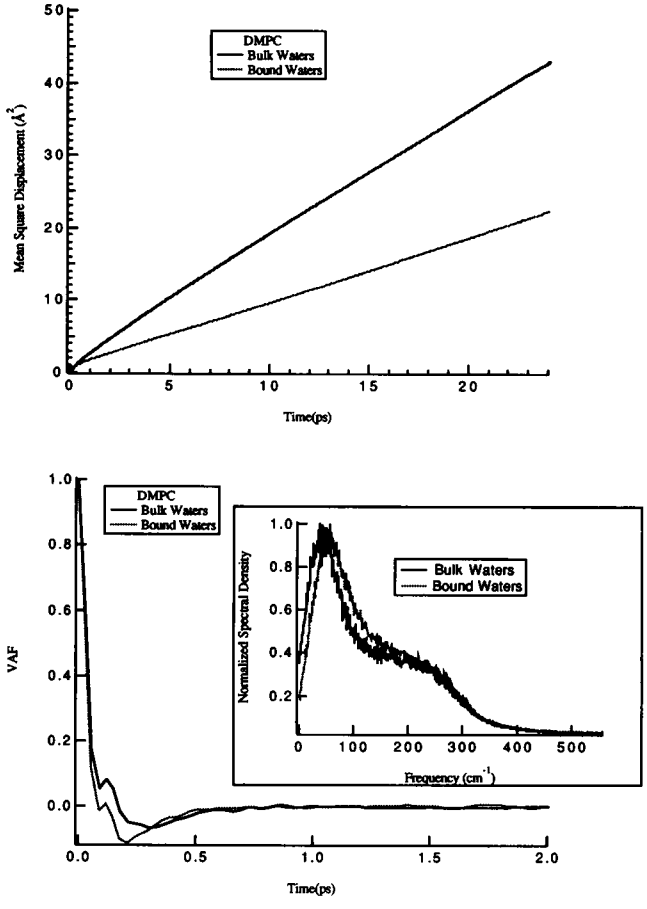

FIGURE 13 Velocity autocorrelation functions (*bottom*) and mean square displacements (*top*) for the bulk and bound waters in the DMPC-based bilayer. The normalized power spectra obtained from the velocity autocorrelation functions are shown as an inset in the *bottom* figure.

the water molecules close to the head groups in DMPC is clearly demonstrated by the pair distribution functions. The orientational polarization profiles are of similar nature for DMPC and DLPE, especially the region of importance from the point of view of hydration repulsion. PMF simulations for the TM and AM ions were carried out to determine the effect of the different water structure on their interactions. The PMF profiles show modest differences due to the presence of clathrates around TM versus hydrogen-bonded water molecules around the AM ions. In particular, the TM profile is weakly attractive at ~8 Å, but then becomes repulsive at ~6 Å, whereas the AM profile is weakly repulsive up to ~3 Å, where it becomes strongly repulsive. Hence, the PMF simulation results do not support our earlier suggestion that the differences in the head group solvation of TM and AM plays a role in the hydration force (Damodaran and Merz, 1993).

Recently, McIntosh and Simon (1993) have examined the subgel phase of DPPC and have broken down the total repulsive pressure in this system into four components given by Eq. 3.

$$P = P_{vsr} + P_{sr} + P_u - P_{vdw} \quad (5)$$

P_{vsr} describes the very short range steric interactions (<4 Å interlamellar spacing (IS)), P_{sr} describes intermediate range interactions (~4–8 Å IS), P_u describes long-range repulsive interactions (>8 Å IS), and P_{vdw} describes favorable van der Waals interactions. The IS given are those used by McIntosh and Simon (1993) for the DPPC system and describe the distance between the *furthest* edge of the two leaflets of the bilayer. The P_{vsr} term arises due to bad steric contacts between bilayers as they are forced to come into close contact with one another (Israelachvili and Wennerstrom, 1992; McIntosh and Simon, 1993). The explanation for the origin of the P_{sr} term is more controversial (Israelachvili and Wennerstrom, 1992; Rand and Parsegian, 1992). It has been suggested that partial orientation of water gives rise to these interactions (Marcelja and Radic, 1976), or that lipid protrusion and the entropic confinement of head groups (Israelachvili and Wennerstrom, 1992) are responsible for P_{sr}. In the case of DPPC, McIntosh and Simon found that the decay length of the P_{sr} for the subgel, gel and liquid crystalline phases are very similar, which suggests that the origin of P_{sr} is similar in all of these phases. From their analysis they suggest that the origin of P_{sr} has to do mostly with the reorientation of water molecules because one might imagine that protrusion and entropic confinement of head groups would be greater in the liquid crystalline phase than in the subgel phase; thus, giving different decay lengths due a different molecular mechanisms for the origin of P_{sr}.

Our PMF profile for two of the TM ions indicates that a broad minimum lies between ~6–10 Å (see Fig. 6), which corresponds to the solvent-separated region along the PMF. Our distances are determined by the nitrogen-to-nitrogen distance, hence, our intermolecular spacings are larger than those defined by McIntosh and Simon by ~2 Å (this assumes that the N-C distance on average contributes ~1 Å to the intermolecular spacing between the two TM ions). Nonetheless, our PMF profile suggests that at distance of ~10 Å (McIntosh and Simon's 4–8 Å) there is a layer of water molecules between the two TM ions. As we move from ~10 to ~7 Å we begin to slowly squeeze out water molecules between the TM ions. Once we get past 7 Å we have removed all water molecules from the space between the two TM ions and we begin to reach the P_{vsr} region. Hence, our results are consistent with water reorientation (or removal) as the molecular origin of P_{sr} (McIntosh and Simon, 1993).

The origin of P_u (>10 Å nitrogen-to-nitrogen distance) does not appear to be due to differences in the solvation of the DLPE and DMPC head groups (compare Figs. 4 and 6), but is likely due to entropic confinement of the head groups, protrusion forces, or undulation forces (Israelachvili and Wennerstrom, 1992; McIntosh and Simon, 1993). Our simulations on DLPE and DMPC indicate (see the VAF section above) that the choline head group is much more dynamic than the ethanolamine head group, so it appears that entropic confinement plays a role. However, we are unable to comment on the role undulation or protrusion might play in P_u due to the short timescale of our simulations.

Finally, we ask the question, "Why do liquid crystalline DMPC and DLPE-based lipid bilayers have very different interlamellar spacings?". We think there are two reasons. (1) The head group of DMPC enjoys much more dynamical freedom than does the DLPE head group due to the lack of hydrogen bond interactions between the choline head group and the phosphate group. This gives rise to a greater P_u term for DMPC because a greater entropic penalty will have to be paid in order to restrain the motion of the DMPC head group region. Because the DLPE head group is already partially immobilized we expect that the entropic penalty is less in this case. (2) At close distance we have found that DLPE can create interlamellar "cross links," which likely stabilize the interaction between two leaflets, although our PMF suggests that the interaction between two AM ions is slightly repulsive at short distances. Another consideration has to do with the electrostatic signature of the DLPE interface. Because the phosphate and ammonium ions are approximately on the same plane (see Fig. 7), it is possible that as two DLPE-based bilayers approach one another the negative and positive regions could align up with one another, resulting in a net stabilizing interaction at small interlamellar spacings.

More generally, we have found from our simulations on DMPC- and DLPE-based bilayers that we have been able to reproduce experimental quantities such as order parameter profiles and probability distributions (Damodaran et al., 1992; Damodaran and Merz, 1993). Moreover, we have been able to obtain molecular level insights that would be difficult to obtain experimentally. This indicates that molecular level simulation of bilayers/solvent systems are reasonably robust and will increasingly provide detailed pictures of the structure, function, and dynamics of these unique molecular assemblies.

We thank the Office of Naval Research for supporting our research efforts on lipid bilayers through grant number N00014–90–3–4002. Bruce P. Gaber has also supplied support and encouragement during the course of this work. Helpful discussions with Sid Simon are also acknowledged. Finally, we thank the Pittsburgh Supercomputer and the San Diego Supercomputer Centers for generous allocations of Supercomputer time.

REFERENCES

Alper, H. E., D. Bassolino, and T. R. Stouch. 1993. Computer simulation of a phospholipid monolayer-water system: the influence of long range forces on water structure and dynamics. *J. Chem. Phys.* 98:9798–9807.

Berendsen, H. J. C., J. R. Grigera, and T. P. Straatsma. 1987. The missing term in effective pair potentials. *J. Phys. Chem.* 91:6289–6271.

Berendsen, H. J. C., J. P. M. Postma, W. F. van Gunsteren, A. D. DiNola, and J. R. Haak. 1984. Molecular dynamics with coupling to and external bath. *J. Chem. Phys.* 81:3684–3690.

Berkowitz, M. L., and K. Raghavan. 1991. Computer simulation of a water/membrance interface. *Langmuir* 7:1042–044.

Blume, A. 1983. Apparent molar heat capacities of phospholipids in aqueous dispersion. Effects of chain length and head group structure. *Biochemistry* 22:5436–5442.

Brasseur, R., Editor. 1990. Molecular Description of Biological Membranes by Computer Aided Conformational Analysis. CRC Press, Boca Raton, FL.

Buckner, J. K., and W. L. Jorgensen. 1989. Energetics and hydration of the constituent ion pairs in tetramethylammonium chloride. *J. Am. Chem. Soc.* 111:2507–2516.

Büldt, G., H. U. Gally, J. Seelig, and G. Zaccai. 1979. Neutron diffraction studies on phosphatidylcholine model membranes. *J. Mol. Biol.* 134: 673–91.

Cevc, G., and D. Marsh. 1985. Hydration of noncharged lipid bilayer membranes: theory and experiments with phosphatidylethanolamines. *Biophys. J.* 47:21*a*. (Abstr.)

Damodaran, K. V., and K. M. Merz, Jr. 1993. Head group - water interactions in lipid bilayers: a comparison between DMPC and DLPE based lipid bilayers. *Langmuir* 9:1179–1183.

Damodaran, K. V., K. M. Merz, Jr., and B. P. Gaber. 1992. Structure and dynamics of the dilauroylphosphatidylethanolamine lipid bilayer. *Biochemistry* 31:7656–7664.

Dang, L. X. 1992. Fluoride-fluoride association in water from molecular dynamics simulations. *Chem. Phys. Lett.* 200:21–25.

Dang, L. X., and P. A. Kollman. 1990. Free energy of association of the 18-crown-6:K+ complex in water: a molecular dynamics simulation. *J. Am. Chem. Soc.* 112:5716–5720.

Dang, L. X., and B. M. Pettit. 1990. A theoretical study of like ion pairs in solution. *J. Phys. Chem* 94:4303–4308.

De Loof, H., S. C. Harvey, J. P. Segrest, and R. W. Pastor. 1991. Mean field stochastic boundary molecular dynamics simulation of a phospholipid in a membrane. *Biochemistry* 30:2099*a*. (Abstr.)

Egberts, E., and H. J. C. Berendsen. 1988. Molecular dynamics simulation of a smectic liquid crystal with atomic detail. *J. Chem. Phys.* 89: 3718–3732.

Finer, E. G., and A. Darke. 1974. Phospholipid hydration studied by deuteron magnetic resonance spectroscopy. *Chem. Phys. Lipids.* 12:1*a*. (Abstr.)

Gennis, R. B. 1989. Biomembranes: Molecular Structure and Function. Springer-Verlag, New York.

Hauser, H., I. Pascher, R. H. Pearson, and S. Sundell. 1981. Preferred conformation and molecular packing of phosphatidylethanolamine and phosphatidylcholine. *Biochim. Biophys. Acta.* 650:21–51.

Heller, H., M. Schaefer, and K. Schulten. 1993. Molecular dynamics simulation of a bilayer of 200 lipids in the gel and in the liquid crystal phases. *J. Phys. Chem.* 97:8343–8360.

Huston, S. E., and P. J. Rossky. 1989. Free energies of association for the sodium-dimethyl phosphate ion pair in aqueous solution. *J. Phys. Chem.* 93:7888–7895.

Israelachvili, J. N., and H. Wennerstrom. 1990. Hydration or steric forces between amphiphilic surfaces? *Langmuir* 6:873–876.

Israelachvili, J. N., and H. Wennerstrom. 1992. Entropic forces between amphiphilic surfaces in liquids. *J. Phys. Chem.* 96:520–531.

Janiak, M. J., D. M. Small, and G. G. Shipley. 1979. Temperature and compositional dependence of the structure of hydrated dimyristoyl lecithin. *J. Biol. Chem.* 254:6068–6078.

Jorgensen, W. L., and J. Tirado-Rives. 1988. The opls potential functions for proteins: energy minimizations for crystals of cyclic peptides and crambin. *J. Am. Chem. Soc.* 110:1657–1666.

Kjellander, R., and S. Marcelja. 1985. Polarization of water between molecular surfaces: a molecular dynamics study. *Chemica Scripta.* 25: 73–80.

Marcelja, S., and N. Radic. 1976. Repulsion of interfaces due to boundary water. *Chem. Phys. Lett.* 42:129–130.

McCammon, J. A., and S. C. Harvey. 1987. Dynamics of Proteins and Nucleic Acids. Cambridge University Press, New York.

McIntosh, T. J. 1990. X-ray diffraction analysis of membrane lipids. *In* Molecular Description of Biological Membranes by Computer Aided Conformational Analysis. CRC Press, Boca Raton, FL. pp. 247–265.

McIntosh, T. J., A. D. Magid, and S. A. Simon. 1989. Range of the solvation pressure between lipid membranes: dependence on the packing density of solvent molecules. *Biochemistry.* 28:7904–7912.

McIntosh, T. J., and S. A. Simon. 1986. Area per molecule and distribution of water in fully hydrated dilauroylphosphatidylethanolamine. *Biochemistry.* 25:4948*a*. (Abstr.)

McIntosh, T. J., and S. A. Simon. 1993. Contributions of hydration and steric (entropic) pressures to the interactions between phosphatidylcholine bilayers: experiments with the subgel phase. *Biochemistry.* 32:8374–8384.

McIntosh, T. J., and S. A. Simon. 1986. Hydration force and bilayer deformation: a reevaluation. *Biochemistry.* 25:4058–4066.

Merz, K. M., Jr. 1992. Analysis of a large database of electrostatic potential derived atomic point charges. *J. Comput. Chem.* 13:749–767.

Pastor, R. W., R. M. Venable, and M. Karplus. 1988. Brownian dynamics simulation of a lipid chain in a membrane bilayer. *J. Chem. Phys.* 89: 1112–1127.

Pastor, R. W., R. M. Venable, and M. Karplus. 1991. Model for the structure of the lipid bilayer. *Proc. Natl. Acad. Sci. USA* 88:892–896.

Pearlman, D. A., D. A. Case, J. C. Caldwell, G. L. Seibel, U. C. Singh, P. Weiner, and P. A. Kollman. 1991. AMBER 4:0. University of California, San Francisco.

Pearson, R. H., and I. Pascher. 1979. The molecular strucutre of lecithin hydrates. *Nature.* 281:499–501.

Pettit, B. M., and P. J. Rossky. 1986. Alkali halides in water: ion-solvent correlations and ion-ion potentials of mean force at infinite dilution. *J. Chem. Phys.* 84:5836–5844.

Raghavan, K., M. R. Reddy, and M. L. Berkowitz. 1992. A molecular dynamics study of the structure and dynamics of water between dilauroylphosphatidylethanolamine bilayers. *Langmuir.* 8:233–240.

Rand, R. P. 1981.[007f] Interacting phospholipid bilayers: measured forces and induced structural changes. *Ann. Rev. Biophys. Bioengin.* 10: 277*a*. (Abstr.)

Rand, R. P., and V. A. Parsegian. 1992. The forces between interacting bilayer membranes and the hydration of phospholipid assemblies. *In* The Structure of Bilogical Membranes. CRC Press, Boca Raton, FL. pp. 251–306.

Ryckaert, J. P., G. Ciccotti, and H. J. C. Berendsen. 1977. Numerical integration of the cartesian equations of motion of a system with constraints: molecular dynamics of n-alkanes. *J. Comput. Phys.* 23:327–341.

Salsbury, N. J., Darke, A., and Chapman, D. 1973. Deuteron magnetic resonance studies of water associated with phospholipids. *Chem. Phys. Lipids.* 8:142*a*. (Abstr.)

Scott, H. L. 1977. Monte Carlo studies of the hydrocarbon region of lipid bilayers. *Biochim. Biophys. Acta.* 469:264*a*. (Abstr.)

Scott, H. L. 1986. Monte Carlo calculations of order parameter profiles in models of lipid-protein interactions in bilayers. *Biochemistry.* 25:6122*a*. (Abstr.)

Scott, H. L., and S.-L. Cherng. 1978. Monte Carlo studies of phospholipid lamellae. Effects of proteins, cholesterol, bilayer curvature and lateral mobility on order parameters. *Biochim. Biophys. Acta.* 510:209*a*. (Abstr.)

Scott, H. L., and S. Kalaskar. 1989. Lipid chains and cholesterol in model membranes: a Monte Carlo study. *Biochemistry.* 28:3687–3691.

Seelig, A., and J. Seelig. 1974. The dynamic structure of fatty acyl chains in a phospholipid bilayer measured by deuterium magnetic resonance. *Biochemistry.* 13:4839–4845.

Seelig, J. 1977. Deuterium magnetic resonance: theory and application to lipid membrances. *Quart. Rev. Biophys.* 10:353–418.

Seelig, J., and J. L. Browning. 1978. General features of phospholipid conformation in membranes. *FEBS Lett.* 92:41*a*. (Abstr.)

Simon, S. A., and T. J. McIntosh. 1989. Magnitude of the solvation pressure depends on dipole potential. *Proc. Natl. Acad. Sci. USA* 86:9263–9267.

Stouch, T. R. 1993. Lipid membrane structure and dynamics studied by all-atom molecular dynamics simulations of hydrated phospholipid bilayers. *Mol. Sim.* 10:335–62.

van der Ploeg, P., and H. J. C. Berendsen. 1982. Molecular dynamics simulation of a bilayer membrane. *J. Chem. Phys.* 76:3271–3276.

van der Ploeg, P., and H. J. C. Berendsen. 1983. Molecular dynamics of a bilayer membrane. *Mol. Phys.* 49:233–248.

Weiner, S. J., P. A. Kollman, D. A. Case, U. C. Singh, C. Ghio, G. Alagona, S. Profeta, and P. Weiner. 1984. A new force field fo molecular mechanical simulation of nucleic acids and proteins. *J. Am. Chem. Soc.* 106:765–784.

Weiner, S. J., P. A. Kollman, D. T. Nguyen, and D. A. Case. 1986. An all atom force field for simulations of proteins and nucleic acids. *J. Comput. Chem.* 7:230–252.

Wiener, M. C., and S. H. White. 1992. Structure of a fluid dioleoylphosphatidylcholine bilayer determined by joint refinement of x-ray and neutron diffraction data. II. Distribution and packing of terminal methyl groups. *Biophys. J.* 61:428–433.

Wiener, M. C., and S. H. White. 1992. Structure of a fluid dioleoylphosphatidylcholine bilayer determined by joint refinement of x-ray and neutron diffraction data. III. Complete structure. *Biophys. J.* 61:434–447.

Yeagle, P. L., and A. Sen. 1986. Hydration and the lamellar to hexagonal ii phase transition of phosphatidylethanolamine. *Biochemistry.* 25: 7518–7522.